COMMUNICATIONS IN COMPUTATIONAL PHYSICS
Vol. **2**, No. 6, pp. 1085-1094

Commun. Comput. Phys.
December 2007

Emissivity Calculations Under DCA-UTA Approximation for NLTE Plasmas

J. Q. Pang*, Z. Q. Wu and J. Yan

Institute of Applied Physics and Computational Mathematics, Laboratory of Computational Physics, P. O. Box 8009-57, Beijing 100088, China.

Received 26 October 2006; Accepted (in revised version) 26 January 2007

Communicated by Zhihong Lin

Available online 15 June 2007

Abstract. A model is developed to calculate emission spectrum from plasmas in non-local-thermodynamic-equilibrium (NLTE). The populations are obtained with a Collisional Radiative Model and the spectrum is calculated with the Unresolved-Transition-Array (UTA) approximation. The present model is applied to the calculation of emissivity from low-, medium- and high-Z plasmas. The integrated emissivity and the spectra are compared with those calculated by other theoretical models. In general speaking, the present results of the mean charge state and emissivity agree well with some theoretical ones while large differences are found when all the theoretical results are included.

PACS: 52.20.Dq, 52.70.-m, 52.77.-j

Key words: Non-local-thermodynamic-equilibrium (NLTE), emissivity, Unresolved-Transition-Array (UTA).

1 Introduction

In plasma diagnostics, optimizing X-ray source design et al, emission spectra for NLTE plasmas may be used. In a hydrodynamic simulation code, the spectrally integrated emissivity provided by the atomic physics model determines the evolution of the electronic and radiation temperatures. The spectrum is itself of interest, as hard X-ray photons can generate target preheating in ICF capsules. As the NLTE condition is universal in laboratory and astrophysical plasma studies, the capability to accurately predict emissivity from NLTE plasmas is of primary interest. Calculation of complete spectra for NLTE plasmas needs detailed atomic structure codes, radiative and collisional processes calculations for numerous ion species, level population models and treating a large number of

*Corresponding author. *Email addresses:* pang_jinqiao@mail.iapcm.ac.cn (J. Q. Pang), wu_zeqing@mail.iapcm.ac.cn (Z. Q. Wu), yan_jun@mail.iapcm.ac.cn (J. Yan)

transitions. Despite these difficulties, we have to tackle these problems because spectral information is an invaluable tool for providing information on the plasma parameters.

In recent years, many codes, such as Fine [1], Hullac [2], Nomad [3], Transpec [4] et al., have been developed to calculate the populations and the spectra from NLTE plasmas. In order to obtain accurate spectra, taking into account all the important configurations as well as high accurate atomic model is required. On the other hand, the unendurable computational time compel us to employ various approximations in atomic or population models. That is why the results from different codes do not agree well. Very recently, a 'virtual workshop' is performed to compare NLTE emissivities produced by widely differing type of atomic physics codes [5]. The workshop shows that even with similar ionizations, the dispersion in emissivity can be enormous. The differences can be orders of magnitude if an otherwise closed shell has been opened. As regards the integrated emissivity, the results of the workshop show roughly a factor from 2-50 scatter which indicates that we should not be surprised at discrepancies between experimental and theoretical emissivities in the design of multi-keV X-ray sources.

Because of the important application of the emission spectra from NLTE plasmas, tests of theoretical model are essential. Accordingly, it is important to provide a method in which the NLTE calculations can be benchmarked against the well-characterized experimental data. In an attempt to reach this goal, some recent experiments in laser-irradiated argon gas bag [6], in laser-produced plasmas on gold targets [7], in inertial confinement fusion (ICF) hohlraums [8], in a simulated coronal plasma environment produced in electron beam ion trap (EBIT) [9] and in laser-heated xenon gas jet plasmas [10] have been performed. Comparisons show that some of the theoretical models have reasonable ionizations compared with the experimental values, but the discrepancies are substantial in some cases. As for the emissivity, some theoretical models can usually reproduce part of the experimental spectra while the remains are in very poor agreements. Although good agreements between experimental spectra and theoretical simulations are not reached, the comparisons give information on what accuracy of theoretical calculations can be reasonably expected. The discrepancies demonstrate that there is still much room to improve the NLTE calculations and more well-determined experiments are needed to check the theoretical models.

In this paper, we develop a model and a corresponding code to calculate the NLTE emission spectra. The code includes selecting configurations, producing all the required atomic parameters, establishing and solving the rate equations to get the populations and using the UTA approximation to obtain the spectra. In the present model, the populations are obtained by a detailed configuration accounting (DCA) collisional radiative model (CRM) [11]. In the population calculations, the steady-state approximation is used. The detailed description of the present CRM is given in our previous publication [11]. In the following section, the theory of the present model will be given. In the third section, the model will be applied to plasmas and the results will be compared with other theoretical ones.

2 Theory

In NLTE plasmas, the ion fractions are determined by the rate equations

$$\frac{dN_i}{dt} = -N_i \sum_j R_{ij} + \sum_j R_{ji} N_j, \quad i = 1,2,\cdots, \tag{2.1}$$

where N_i is the population of the i-th configuration and R_{ij} is the rate coefficient from the i-th configuration to the j-th one through photoionization, electron impact ionization, electron impact excitation, spontaneous radiation, autoionization or their inverse processes. Configuration averaged rate coefficients are used in the rate equations. The cross sections are calculated based on the first order perturbation theory. Wave functions required in cross section calculations are obtained by Hatree-Fock-Slater (HFS) self-consistent-field (SCF) model [12]. The collisional processes are calculated using the distorted-wave approximation with the exchange correction (DWE) in [13]. The results of the atomic processes are investigated in [14].

In the present model, the non-relativistic configurations are adapted in the rate equations. However, in the calculation of the spectrum, the spin-orbit splitting should be included. The distribution of the relativistic configurations within the same non-relativistic configuration is statistical. The relative populations of the relativistic configurations within the same non-relativistic configuration are determined by Boltzmann distribution,

$$N_{ir} = N_i \frac{g_{ir}}{u_i} e^{-\frac{\chi_{ir}}{kT}}, \qquad u_i = \sum_r g_{i,r} e^{-\frac{\chi_{i,r}}{kT}}, \tag{2.2}$$

where N_{ir} is the population of the r-th relativistic configuration belong to the i-th non-relativistic configuration. χ_{ir} and g_{ir} are the configuration-averaged energy and the statistic weight of the configuration (ir) respectively. The configuration-averaged energy of the relativistic configurations can be estimated rapidly from the SCF energy levels database [12]. The database is constructed from the energy level and quantum defects of some bound orbits and continuum orbits, which have already been calculated before from the SCF method and are arranged within different channels for all ionic stages of an element.

With the ion population obtained by solving the rate equations, i.e. Eq. (2.1), the emission coefficient will be calculated. The UTA approximation is adapted to calculate the emissivity. In the UTA approximation, each configuration-configuration transition array is characterized by the average quantities such as total intensity, average transition energy and variance. Since the detail descriptions of the present UTA codes have been given elsewhere [15,16], here we only emphasize one point. In our calculation, the transition energies, oscillator strength, and variance are evaluated using the relativistic wave functions obtained based on the Dirac-Slater SCF potential. Atomic data are calculated within the framework of quantum defect theory (QDT) [17,18]. Therefore, a huge number of atomic data and the UTA parameters of configurations with high principle numbers can be obtained by interpolations within channels. The emission includes three kinds of

transitions, i.e., the spontaneous emission, the radiative recombination and the free-free transition

$$j(h\nu)=\sum_{i'c'}N_{i'c'}\frac{2\Delta E^3_{i'c',ic}}{h^2c^2}\sigma^{bb}_{i'c',ic}(h\nu)+N_e\sum_{i'c'\varepsilon e}N_{i'c'}\sigma^{fb}_{ic,i'c'\varepsilon e}(h\nu)\frac{Vf(V)dV}{4\pi}\cdot h\nu$$
$$+NN_e\int_{V_{\min}}^{\infty}f(V)VdVh\nu d\sigma_{ff}, \tag{2.3}$$

where $\Delta E_{i'c',ic}$ is the transition energy, $\sigma^{bb}_{i'c',ic}(h\nu)$ is the cross section of the spontaneous emission, $f(V)$ is the distribution function of free electrons, $\sigma^{fb}_{ic,i'c'\varepsilon e}$ is the cross section of radiative recombination, N, $N_{i'c'}$ and N_e are the total ion number density, the population of the i'-th configuration and the free electron density, respectively, $d\sigma_{ff}$ is the differential cross section of bremsstrahlung. The free electrons are in the Maxwellian distribution.

The cross section of the spontaneous emission is given by

$$\sigma^{bb}_{ic,i'c'}(h\nu)=\frac{\pi he^2}{mc}f_{cc'}L(h\nu), \tag{2.4}$$

where f is the configuration averaged transition oscillator strength,

$$f_{cc'}=q_\alpha(1-\frac{q_\beta}{g_\beta})f_{\alpha\beta},\qquad f_{\alpha\beta}=\frac{2m}{3h\nu g_\alpha}|\langle\alpha\|T\|\beta\rangle|^2,$$

and $L(h\nu)$ is the Voigt profile [19],

$$L(h\nu)=\frac{1}{\Gamma}\sqrt{\frac{\ln 2}{\pi}}H(a,v),\qquad H(a,v)=\frac{a}{\pi}\int_{-\infty}^{+\infty}\frac{e^{-x^2}dx}{a^2+(v-x)^2},$$

the line profile is determined by UTA width, the natural width in Lorentz shape, and the Doppler broadening in Gaussian shape. The line broadening is very important in the spectrum calculation because the line transfer is sensitive to the line profile.

The configuration averaged photoionization cross section is given by

$$\sigma^{bf}_{ic}(h\nu)=\sum_{i'c'\varepsilon e}\sigma^{bf}_{ic,i'c'\varepsilon e}(h\nu)=\frac{\pi he^2}{mc}\sum_\alpha q_\alpha\frac{df_{\alpha,\varepsilon e}}{d\varepsilon},$$

where

$$f_{\alpha,\varepsilon e}=\frac{2m}{3h\nu g_\alpha}|\langle\alpha\|T\|\varepsilon e\rangle|^2.$$

The cross section of the inverse process radiative recombination is obtained by means of the principle of detailed balance

$$\sigma^{fb}_{i'c'\varepsilon e,ic}(h\nu)=\frac{g_{ic}}{g_{i'c'}}\frac{h^2\nu^2}{m^2v^2c^2}\sigma^{bf}_{ic,i'c'\varepsilon e}(h\nu). \tag{2.5}$$

Table 1: Definition of cases.

Cases	Ar1	Ar2	Ge1	Ge2	Ba	Au
$N_e(cm^{-3})$	$3*10^{21}$	10^{20}	10^{20}	$3*10^{22}$	10^{20}	$6*10^{20}$
$T_e(eV)$	3000	200	400	400	250	2200
Spectral range(eV)	2500-5000	0-5000	0-3000	0-3000	800-2500	2000-6000

The differential cross section of bremsstrahlung is obtained using the Classical Kramer Formula with Guant factor

$$d\sigma_{ff} = \frac{16\pi}{3\sqrt{3}}\left(\frac{e^2}{\hbar c}\right)^3 \frac{Z^2h^2}{2m\varepsilon_2}\frac{dv}{v}g_{ff}(v), \tag{2.6}$$

where Z is the charge state of the ion, ε_2 is the energy of the initial continuum electron and g_{ff}, the Guant factor with Born-Elwert approximation [20]

$$g_{ff} = \frac{\sqrt{3}}{\pi}\frac{v_2}{v_1}\frac{1-e^{-2\pi Ze^2/\hbar v_2}}{1-e^{-2\pi Ze^2/\hbar v_1}}\ln\left(\frac{v_2+v_1}{v_2-v_1}\right),$$

where v is the velocity of the continuum electron.

3 Results and discussions

In order to check the present code, we choose the cases as the same as the test cases in the 'virtual workshop' [5] and compared the results with other theoretical ones. The cases that we calculated are listed in Table 1. All the cases are steady-state, optically thin and with no radiation reabsorption.

The results of ionization and emissivity are shown in Figs. 1 and 2 along with those of other theoretical models such as Hullac [2], Nomad [3], Nohel2e.2 [5], Fine [1] and Transpec.averroes [4,20,21]. Hullac and Fine are fully relativistic DCA models, Nomad is a detailed-level-accounting (DLA) model, Transpec.averroes is a non-relativistic DCA model with super-transition-array approximation in spectrum calculations, Nohel is an average atom (AA) model without 2e processes while Nohel2e.2 includes two-electron processes. Hullac.1 and 2 mean different options for solving the rate equations and different configuration space. The data of the other theoretical models come from the third NLTE workshop [5].

Fig. 1 shows the comparison of the mean ionization degree. In Fig. 1, the solid circle represents the present results and the others are the compared data. The symbol of the elements, the electron temperature Te and density Ne are shown. The number beside the elements is the largest difference among the data. For the Au case, the data in the figure are the real ones minus 25 (which is the meaning of -25). The number in the brackets beside the element symbol is the largest difference of the data except for the one of Nohel.

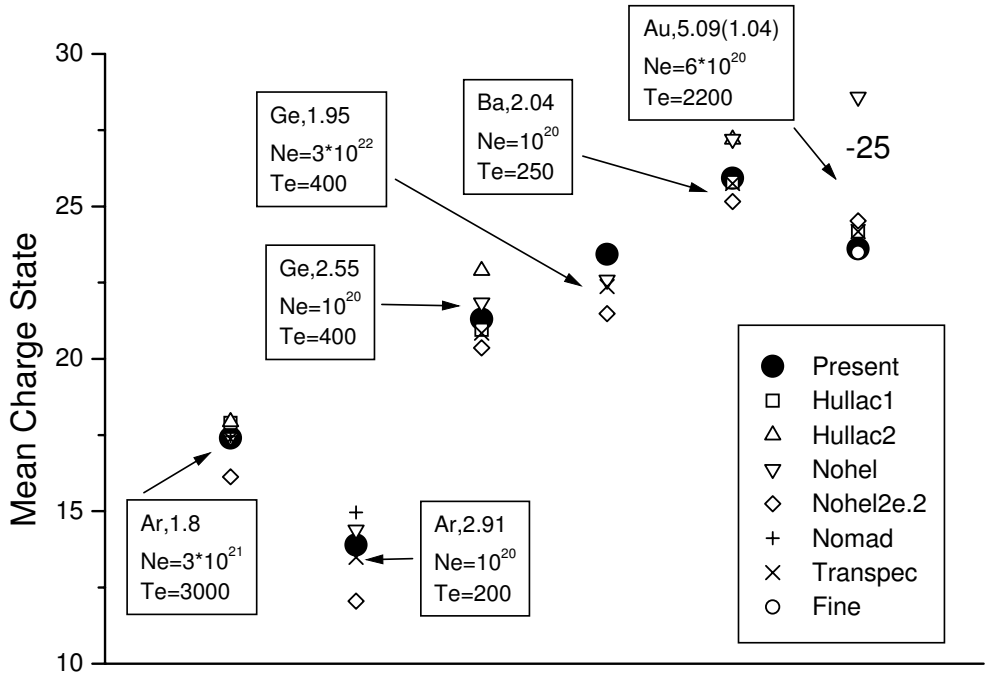

Figure 1: The mean charge states of different plasmas for different codes.

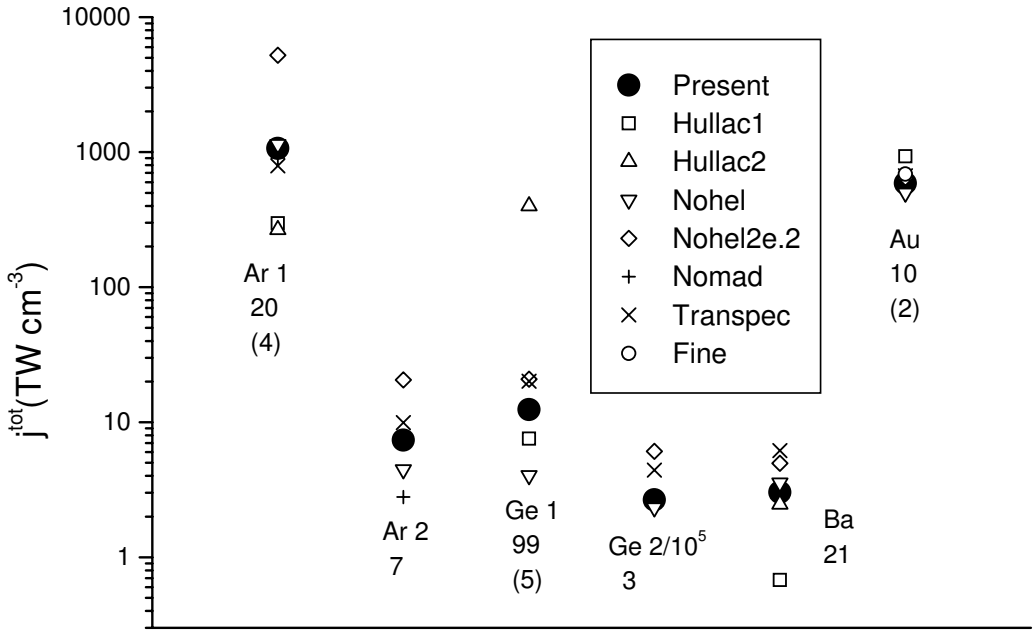

Figure 2: The total spectrally integrated emissivities.

Generally speaking, the present results of the mean ionization stage agree well within 2 degree with all the other theoretical ones. For all the cases, the present values of the mean charge state always have good agreements with those of Hullac.1 and Transpec, the difference in the mean charge is smaller than 0.5. Hullac.2 always gives a much higher ionization degree than the others except for the Ba and Au case. For the Ba and Au case, Nohel gives a higher mean charge state, while Nohel2e.2 gives a lower ionization. Since Nohel2e.2 is a screened hydrogenic average atom model using simple formulae to describe the atomic parameters, the results are not as accurate as the other models. Huallac.1 and 2 have different ionization possibly due to the differences in configuration space available.

Fig. 2 shows the total emissivity j^{tot} integrated over the corresponding spectrum range listed in Table 1. As in Fig. 1, the solid circle is the present results and the others are the compared data. The cases are defined in Table 1. The numbers under the elements are the factor in the scatter of the data and the ones in brackets are the factor in the scatter except for the largest result. For the Ge2 case, the virtual data are the ones in the figure times 10^5. From the comparison, we can see that the results of integrated emissivity agree poorly for all the models. The large scatter in emissivity indicates that the populations of excited configurations calculated by different model are much different. It is necessary to investigate further in NLTE population calculations.

It is surprising that the dispersion in total emissivity can be so enormous. To investigate the emissivity in more detail, the spectrum-resolved emission should be compared.

As examples, the present spectra are compared with those of other theoretical models in Figs. 3 and 4. Fig. 3 shows the spectrum-resolved emission of the Ge1 case. Since the spectra in Ref. [5] are obtained by convoluting the original data with an additional normalized Gaussian profile of width 30 eV, in order to compare with these spectra, an additional width 30 eV of Gaussian profile is added to the present Ge1 spectra. After convoluting with the 30 eV Gaussion profile, the difference in emissivity mainly comes from the peaks around 500 eV and those around 1400 eV which come from the M-shell and the L-shell transitions, respectively. The features of the spectrum from the three models are much alike. However, the details are different. Transpec gives higher intensity than those of Hullac1 and the present code in the photon energy range lower than 1000 eV. In the range larger than 1000 eV, the present model gives a little larger intensity than that of Transpec. It seems that there are more configurations with the L-shell holes in the present model than in Transpec. To explain these differences, more details in the calculations are required.

In Fig. 4, the spectra for the Au case are compared with those of Fine. The dotted line is the result of Fine. The solid thin line is our original spectrum. The thick solid line is the present result after convoluted with 30 eV. The spectrum is also due to the M-shell transitions. The main features of the two spectra are similar. However, the positions and intensities given by the two models are a little different. The main difference between the present spectrum and Fine's is the peak between 3500 to 4300 eV which comes from the $n=5$ shell to the $n=3$ shell transitions. The present code gives lower intensity than Fine,

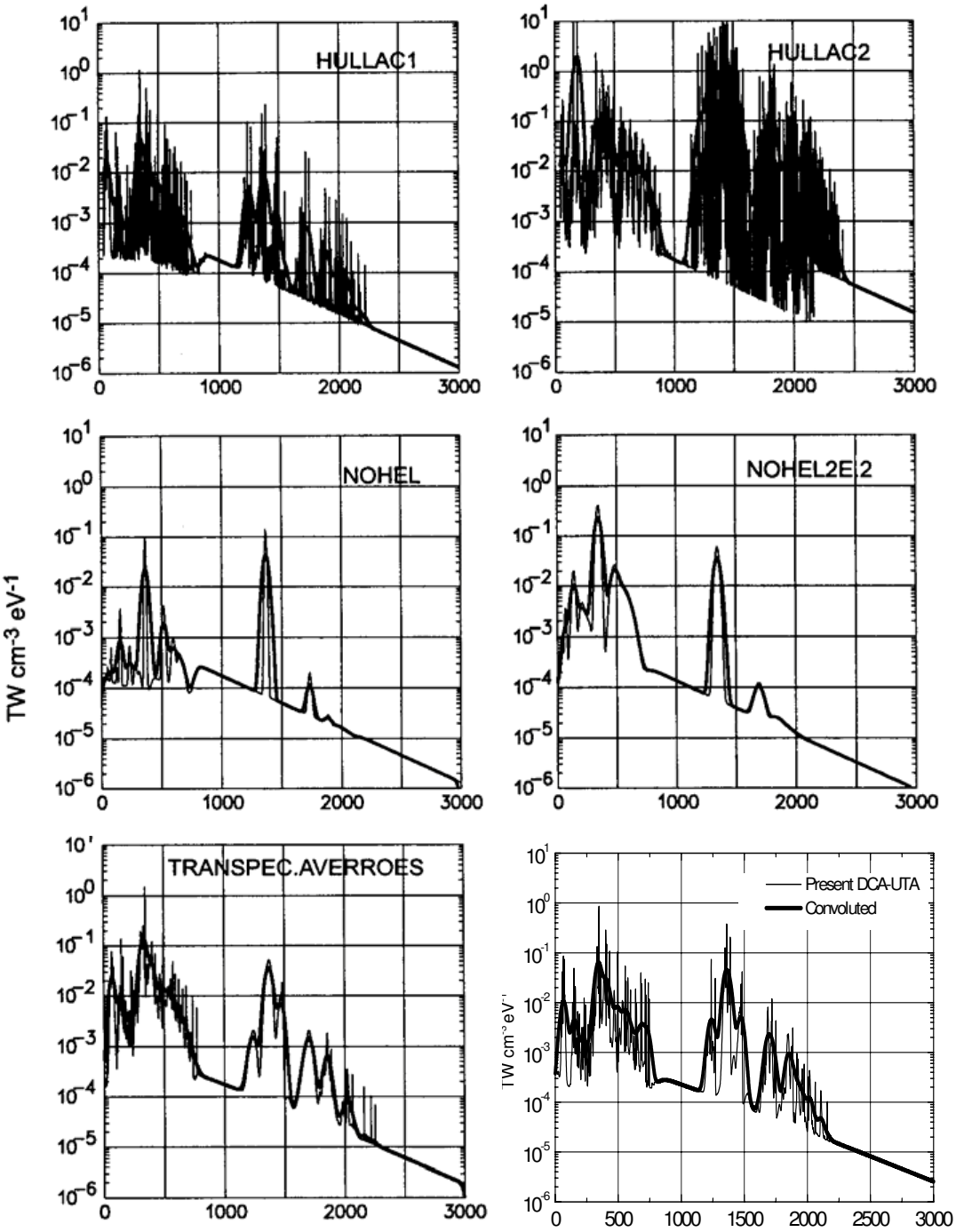

Figure 3: Total emissivity in TW cm^{-3} eV^{-1} vs. photon energy in eV, case Ge1.

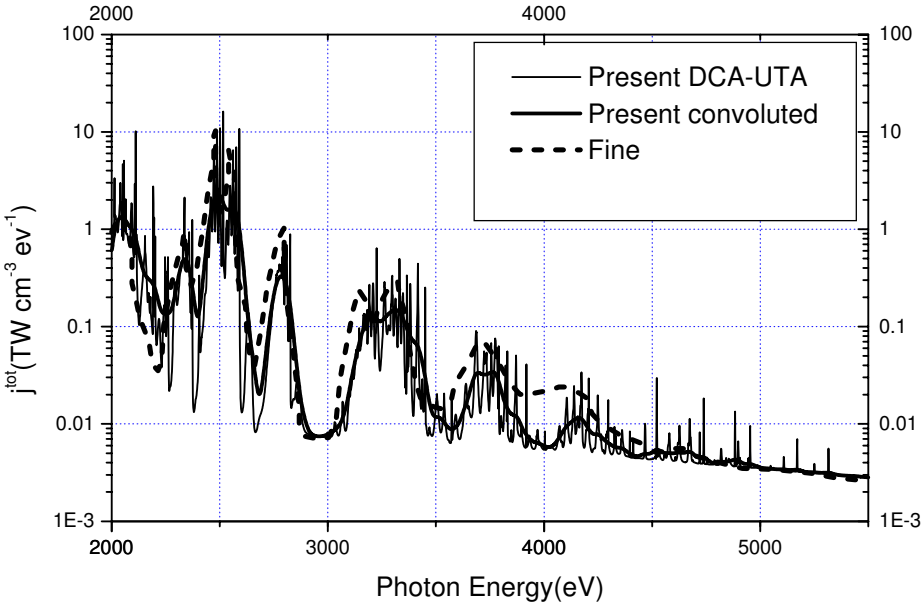

Figure 4: Total emissivity in TW cm^{-3} eV^{-1} vs. photon energy in eV, case Au.

which may indicate that the rates of excitation to the $n=5$ shell are smaller in the present calculation compared to Fine's.

4 Summary

We have developed a model and the corresponding codes to calculate populations and emission spectra for the NLTE plasmas. From the above comparisons, we can see that the present results of the mean ionization degree and emissivity agree well with those of Hullac.1, Transpec and Fine in general. However, large differences are found in emissivity when the other theoretical models are included. We can also see that there is scatter in the integrated emissivity even if the ionization degrees are almost the same, which indicates that the populations are different although the ionizations are the same. When the deviation in the mean ionization is obvious, the dispersion in emissivity is more enormous. The intensity of emission is determined by two factors: the number of the excited state in the radiative process and the probability of the spontaneous radiation. In order to predict the emissivity correctly, the populations should be accurately calculated at first. The populations of excited states may differ by larger factors. The spontaneous probability calculated by different code can also have large deviation. As the emission is determined by excited levels, it is necessary to compare not only the mean ionization but also the populations of excited configuration obtained by different models. Since here we only have information on ionization, integrated emissivity and the spectra from the

other theoretical calculations, it is difficult to explain why there is so large difference in emissivity.

By considering the large spread in the emissivity from various codes and since no benchmark can be obtained, some experimental emission spectra are urgently needed to test the theoretical models.

Acknowledgments

This work was supported by the National Basic Research Program (No. 2005CB724500), National Natural Science Foundation of China (Grant Nos. 10674021 and 10604011), and the Science and Technology Funds of Chinese Academy of Engineering Physics (Grant Nos. 20050215 and 20060215).

References

[1] J. Abdalah, R. E. H. Clark, D. P. Kilcrease, G. Csanak, C. J. Fontes, in: A. L. Osterheld, W. H. Goldstein (Eds.), Atomic Processes in Plasmas, Proceedings of the Tenth Topic Conference, AIP Conference Proceedings, San Francisco, CA, New York, AIP, 1996, pp. 381, 131.
[2] A. Bar-Shalom, M. Klapisch, J. H. Oreg, J. Quant. Spectrosc. Radiat. Transfer 71 (2001) 169.
[3] Y. V. Ralchenko, Y. Maron, J. Quant. Spectrosc. Radiat. Transfer 71 (2001) 609.
[4] O. Peyrusse, J. Quant. Spectrosc. Radiat. Transfer 51 (1994) 281.
[5] C. Bowen, A. Decoster, C. J. Fontes, K. B. Fournier, O. Peyrusse, Y. V. Ralchenko, J. Quant. Spectrosc. Radiat. Transfer 81 (2003) 71.
[6] S. H. Glenzer, K. B. Fournier, C. Decker, B. A. Hammel, R. W. Lee, L. Lours, B. J. MacGowan, A. L. Osterheld, Phys. Rev. E 62 (2000) 2728.
[7] S. H. Glenzer, W. Rozmus, B. J. MacGowan, K. G. Estabrook, J. D. De Groot, G. B. Zimmerman, H. A. Baldis, J. A. Harte, R. W. Lee, E. A. Williams, B. G. Wilson, Phys. Rev. Lett. 82 (1999) 97.
[8] S. H. Glenzer, K. B. Fournier, B. G. Wilson, R. W. Lee, L. J. Suter, Phys. Rev. Lett. 87 (2001) 045002.
[9] K. L. Wong, M. J. May, P. Beiersdorfer, Phys. Rev. Lett. 90 (2003) 235001.
[10] C. Chenais-Popovics, V. Malka, J. C. Gauthier, Phys. Rev. E 65 (2002) 046418.
[11] Z. Q. Wu, J. Q. Pang, G. X. Han, J. Yan, J. Quant. Spectrosc. Radiat. Transfer 87 (2004) 367.
[12] R. D. Cowan, The Theory of Atomic Structure and Spectra, University of California Press, Berkeley, CA, 1981, pp. 176, 406.
[13] V. P. Shevelko, L. A. Vainstein, Atomic Physics for Hot Plasmas, IOP Publishing Ltd, 1993.
[14] Z. Q. Wu, Nucl. Phys. Rev. 19 (2002) 161 (in Chinese).
[15] J. Yan, Y. B. Qiu, Phys. Rev. E 64 (2001) 056401.
[16] J. Yan, Z. Q. Wu, Phys. Rev. E 65 (2002) 066401.
[17] C. M. Lee, Phys. Rev. A 10 (1974) 584; Acta Phys. Sin. 29 (1980) 419.
[18] J. Yan, Y. Z. Qu, L. Voky, J. M. Li, Phys. Rev. A 57 (1998) 997.
[19] S. C. Li, Physics of High Temperature Radiation and the Quamtum Theory of Radiation, Publishing House of National Defence Industry, Beijing, 1992 (in Chinese).
[20] O. Peyrusse, J. Phys. B 33 (2000) 4303.
[21] O. Peyrusse, J. Quant. Spectrosc. Radiat. Transfer 71 (2001) 571.